



Contents lists available at ScienceDirect

## International Journal of Fatigue

journal homepage: [www.elsevier.com/locate/ijfatigue](http://www.elsevier.com/locate/ijfatigue)

## Crack growth-based fatigue-life prediction using an equivalent initial flaw model. Part II: Multiaxial loading

Zizi Lu, Yibing Xiang, Yongming Liu \*

Clarkson University, Potsdam, NY 13699, USA

## ARTICLE INFO

## Article history:

Received 24 February 2009

Received in revised form 18 May 2009

Accepted 8 July 2009

Available online xxx

## Keywords:

Life prediction

Multiaxial fatigue

Crack growth

Critical plane

EIFS

## ABSTRACT

A general methodology is proposed in this paper for fatigue-life prediction using crack growth analysis. This is the part II of the paper and focuses on the fatigue-life prediction under proportional and nonproportional multiaxial loading. The proposed multiaxial fatigue-life prediction is based on a critical plane-based multiaxial fatigue damage model and the Equivalent Initial Flaw Size (EIFS) concept. An equivalent stress intensity factor under general multiaxial proportional and nonproportional loading is defined. The fatigue life is predicted by integration of the crack growth rate curve from the EIFS to the critical crack length. The proposed model can automatically adapt for different materials experiencing different local failure modes. The numerical fatigue-life prediction results calculated by the proposed approach are validated with experimental data for a wide range of metallic materials available in the literature. Reasonable agreements are observed between the model predictions and the experimental observations under proportional and nonproportional loading.

© 2009 Elsevier Ltd. All rights reserved.

### 1. Introduction

Many mechanical and structural components experience multi-axial cyclic loadings in service, e.g. the mast in a helicopter, railroad wheels, turbine blades, drive shafts, etc. [1–3]. Anisotropy of materials can also cause multiaxial fatigue problem even under the uniaxial loading, e.g. multidirectional composite laminate [4]. The multiaxial fatigue problem is more difficult due to its complex stress states, nonproportional loading histories and various initial crack orientations [5]. Although extensive efforts have been made in the past decades there is no universally accepted model available. Several reviews and comparisons of existing multiaxial fatigue models can be found in [6–10].

Fatigue-life prediction can be generally classified into two approaches: the stress (strain)-life approach and the fracture mechanics-based approach. Most existing multiaxial fatigue theories were developed based on the stress (strain)-life approach. A brief review is given below.

The stress based approaches can be classified into four categories: empirical equivalent stress model, stress invariants model, average stress model, and critical plane-based model [5]. Gough and Pollard [11,12] suggested two empirical equivalent stresses for multiaxial fatigue analysis of metals under combined proportional bending and torsion. Their proposed criteria does not address nonproportional loading. Lee [13] presented an empirical

design criterion for fully reversed nonproportional torsion and bending by modifying Gough's ellipse quadrant [11]. The drawback of Lee's criterion is that many experimental data is required for model calibration. Sines [14] developed a high-cycle fatigue criterion using the mean values of the shear and normal stresses. This model was only used for ductile materials under the fatigue limit regime.

Various models based on stress invariants were proposed in [15–20]. Sines [15] used the stress invariants for high-cycle fatigue analysis and introduced a linear dependence of the bending limit upon a superimposed static normal stress. In his proposed model [15], the ratio of fatigue limits in torsion and in fully reversed bending remains constant for all metals, which is not supported by experimental results. Crossland [17] suggested a similar criterion as the Sines' model [15], but considered the influence of the hydrostatic stress. The uniqueness of the torsion fatigue limit is correctly reproduced. Kakuno and Kawada [19] proposed a design formula by separating the effects of the amplitude and the mean value of the hydrostatic stress. The proposed method [19] is not applicable for all nonproportional loading conditions. One major limitation of the stress invariant approach is that it cannot predict the orientation of the initiated fatigue crack [7], which is another important characteristic of the multiaxial fatigue problem.

Another approach is the average stress approach, which uses the average stress within an area/volume as the damage indicator. Papadopoulos et al. [7] proposed an average stress approach using the average value of the stress components involving the critical point. This model is limited to hard metals for which the ratio of

\* Corresponding author. Tel.: +1 315 268 2341; fax: +1 315 268 7985.  
E-mail address: [yliu@clarkson.edu](mailto:yliu@clarkson.edu) (Y. Liu).

$t_{-1}/f_{-1}$  (the fully reversed torsion fatigue limit over the fully reversed bending fatigue limit) is between  $1/\sqrt{3}$  and 0.8. Another limitation of the model is that nonproportional loading has no effect on the life prediction which is not consistent with experimental observations [6]. Sonsino and Crubisic [21] observed that the decrease of fatigue life under out-of-phase strains was caused by of the change of principal strain directions, which results in an interaction of the deformations in all directions on the surface. This interaction could be accounted for by the arithmetic mean of the shear amplitudes acting in all interference planes on the surface. Sonsino and Crubisic's method is originally proposed for sinusoidal loading only. Liu and Zenner [22] also introduced a criterion based on the space averages to explain the multiaxial fatigue behavior.

In the past decades, fatigue-life prediction criteria based on the critical plane approach became widely used because they generally predicted the fatigue damage more accurately [23]. The critical plane approach is based on the physical observations that fatigue cracks initiate and grow along certain planes in the material. This concept was firstly proposed by Stanfield [24], and has been developed since then by other researchers [25]. Various critical plane-based models that use the  $S-N$  (e- $N$ ) curves have been proposed. Findley [26] and Matake [27] presented a similar criterion for high-cycle multiaxial fatigue analysis using the shear stress amplitude and the maximum value of the normal stress on the critical plane. Findley [26] determined the critical plane by maximize a linear combination of the shear stress amplitude and the maximum value of the normal stress. Matake [27] defined the critical plane as the one experiencing the maximum shear stress amplitude. McDoarmid [28] used the concept of case A and case B cracks introduced by Brown and Miller [29] and proposed a generalized failure criterion that takes the crack initiation modes into consideration. However, this criterion is limited to the range of loading conditions and does not explain the mean stress effect. Fatemi and Socie [30] modified the parameter in the Brown and Miller's approach [29] to account for the additional cyclic hardening during nonproportional loading. Carpinteri and Spagnoli [8,31,32] proposed that the critical plane orientation is determined by the principal stress directions through a weight average function under nonproportional loading. Liu and Mahadevan [5] proposed a unified multiaxial fatigue damage model based on the critical plane approach. One unique property of the proposed model is that the critical plane is related to material ductility and varies for different local failure modes. The applicability of the proposed model [5] is significantly improved.

Multiaxial fatigue models based on the  $S-N$  curve approach are not suitable for damage tolerance analysis, which is based on the fracture mechanics. In this paper, a multiaxial fatigue life model is proposed based on the crack growth analysis. The proposed methodology integrates a previously developed multiaxial fatigue model [33] and a general life prediction methodology based on the Equivalent Initial Flaw Size (EIFS) concept [34]. The proposed multiaxial model is applicable to a wide range of ductile and brittle metals. It does not require solving the inverse crack growth problem, which makes the computation very efficient. A wide range of experimental data for different metallic materials is used for model validation.

A similar method was proposed by Döring et al. [35], i.e. the short crack model is based on the critical plane concept and a starter crack length  $a_0$  is used for the fatigue-life prediction. The starter crack length in [35] is determined by backward integration of the Paris type crack growth equation. The proposed EIFS concept is different from the commonly used backward integration and is easy to be calculated, i.e. no iterative calculation is required. Also, it is independent of applied load level, which is one of common drawbacks of the backward integration method [34]. As for the critical plane method, the one used in [35] is based on the critical plane concept proposed by Brown and Miller [29] and Fatemi and Socie

[30]. The fatigue damage is accumulated in the same way for different materials under the same stress state and their applicability generally depends on the material's properties. In our paper, the critical plane depends on both the stress state and the material properties. One of the advantages of the proposed critical plane method is that it can automatically adapt for different materials experiencing different local failure modes. Detailed comparison of the proposed critical plane method and other critical plane method can be found in [5,36].

## 2. Proposed methodology

### 2.1. Mixed mode fatigue crack growth

The critical plane-based model for multiaxial fatigue damage analysis proposed by Liu and Mahadevan [33] is summarized below. Detailed derivation and validation can be found in the referred article. The general fatigue limit criterion under multiaxial loading is expressed as

$$\sqrt{\left(\frac{\sigma_c}{f_{-1}}\right)^2 + \left(\frac{\tau_c}{t_{-1}}\right)^2} + A\left(\frac{\sigma_H}{f_{-1}}\right) = B \quad (1)$$

where  $\sigma_c$  and  $\tau_c$  are the normal stress range and shear stress range acting on the critical plane for both nonproportional loading and proportional loading, respectively.  $\sigma_H$  is the hydrostatics stress amplitude.  $A$  and  $B$  are the material parameters which can be determined from uniaxial and torsional fatigue limits. Material parameters  $A$ ,  $B$ , and  $\gamma$  are listed in Table 1. The material parameter  $s = t_{-1}/f_{-1}$  is related to the material ductility and affects the critical plane orientation. In Eq. (1), the ranges of the stress components  $\sigma_c$  and  $\tau_c$  are evaluated by taking the difference of the maximum value and the minimum value on the critical plane. For general nonproportional loading case, this is done by enumeration. Details can be found in [35] using the proposed critical plane method. In this paper, only the constant proportional and nonproportional loading is considered. Therefore, the ranges of the stress components are calculated using the maximum and minimum value during one external loading cycle.

For brittle materials, the critical plane is close to the maximum normal stress amplitude plane. For ductile materials, the critical plane is close to the maximum shear stress amplitude plane. Thus, this model can automatically adapt for different failure modes, i.e. tensile or shear dominated failures [36]. The critical plane is load path-dependent since different loading paths result in different maximum normal stress plane. Therefore, the proposed model includes the loading path effect and the nonproportional loading influence on the fatigue life, which has been discussed in detail in [33].

Kitagawa diagram [37] and El Haddad's model [38] is used to link the multiaxial fatigue limit criteria to the fatigue crack growth threshold stress intensity factor. The fatigue limit can be expressed using the threshold stress intensity factor and a fictional crack length  $a$  [33] as

$$f_{-1} = \frac{K_{I,th}}{\sqrt{\pi a}} \quad (2)$$

**Table 1**  
Material parameters for fatigue limit criterion.

Material property	$s = \frac{t_{-1}}{f_{-1}} \leq 1$	$s = \frac{t_{-1}}{f_{-1}} > 1$
$\gamma$	$\cos(2\gamma) = \frac{-2 + \sqrt{4 - 4(1/s^2 - 3)(5 - 1/s^2 - 4s^2)}}{2(5 - 1/s^2 - 4s^2)} \leq 1$	$\gamma = 0$
$A$	$A = 0$	$A = 9(s^2 - 1)$
$B$	$B = [\cos^2(2\gamma)s^2 + \sin^2(2\gamma)]^{\frac{1}{2}}$	$B = s$

where  $K_{I,th}$  is the threshold stress intensity factor under mode I loading. A similar formula can be also expressed for mode II loading.

$$t_{-1} = \frac{K_{II,th}}{\sqrt{\pi a}} \quad (3)$$

where  $K_{II,th}$  is the threshold stress intensity factor under mode II loading.

An infinite plate with a centered through crack of length  $2a$  is used to illustrate how to derive the effective stress intensity factor under general multiaxial loading. The remote tensile stress and remote shear stress on an infinite plate with a zero stress ratio have ranges of  $\sigma$  and  $\tau$ , respectively. The range of the mode I stress intensity factor is

$$K_I = \sigma\sqrt{\pi a} \quad (4)$$

The range of the mode II stress intensity factor is

$$K_{II} = \tau\sqrt{\pi a} \quad (5)$$

Substitute Eqs. (2)–(5) into Eq. (1) and use the results in Table 1, one can obtain

$$\sqrt{\left(\frac{k_1}{K_{I,th}}\right)^2 + \left(\frac{k_2}{K_{II,th}}\right)^2} + A\left(\frac{k^H}{K_{I,th}}\right) = B \quad (6)$$

where  $k_1$ ,  $k_2$  and  $k^H$  are loading-related parameters having the same units as the stress intensity factor. For proportional multiaxial loading, they can be expressed as the range of the corresponding stress intensity factor's range, i.e.

$$\begin{cases} k_1 = \max(k_{1,t}) - \min(k_{1,t}) \\ k_2 = \max(k_{2,t}) - \min(k_{2,t}) \\ k_t^H = k_1/3 \end{cases} \quad (7)$$

$$\text{and } \begin{cases} k_{1,t} = \frac{K_{I,t}}{2}(1 + \cos 2\alpha) + K_{II,t} \sin 2\alpha \\ k_{2,t} = -\frac{K_{I,t}}{2}(\sin 2\alpha) + K_{II,t} \cos 2\alpha \\ k_t^H = \frac{K_{I,t}}{3} \end{cases} \quad (8)$$

where the critical plane orientation  $\alpha$  can be expressed as

$$\alpha = \beta + \gamma \quad (9)$$

where  $\beta$  is the maximum normal stress amplitude plane orientation at the far field.  $\gamma$  is listed in Table 1. A schematic representation of the critical plane orientation is shown in Fig. 1.

An equivalent stress intensity factor can then be expressed as

$$K_{mixed,eq} = \frac{1}{B} \sqrt{(k_1)^2 + \left(\frac{k_2}{S}\right)^2} + A(k^H)^2 = K_{I,da/dN} = f\left(\frac{da}{dN}\right) \quad (10)$$

where  $f\left(\frac{da}{dN}\right)$  is the crack growth curve obtained under mode I loading. The quantity of  $s$  in 10 is redefined as  $s = \frac{K_{II,da/dN}}{K_{I,da/dN}}$ . The value of  $s$  depends on the material and its typical value for ductile materials is

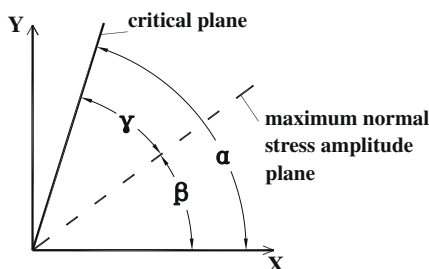


Fig. 1. Orientation of critical plane and maximum normal stress plane.

about 0.55–0.7 and the ratio is larger than 1.0 for brittle materials. This value for several materials has been reported in [33]. The original discussion for this ratio and its meaning can be found in [5,36]. The parameters in Table 1 can be used in Eq. (10) to find a fatigue crack growth rate prediction under mixed-mode loading. The equivalent stress intensity factor (Eq. (10)) can be used to predict general mixed-mode crack growth rate using measured mode I crack growth curve [33]. For prediction corresponding to a general crack growth rate  $da/dN$ , the threshold stress intensity factor may be replaced by the stress intensity coefficients at the specific crack growth rate ( $K_{I,da/dN}$  and  $K_{II,da/dN}$ ). The applicability of the proposed model to the mixed-mode crack analysis has been demonstrated and validated in [33] under various loading conditions.

## 2.2. Life prediction based on EIFS

In part I of this paper, a general fatigue-life prediction methodology based on the Equivalent Initial Flaw Size (EIFS) concept has been proposed. The EIFS is determined by

$$a_i = \frac{1}{\pi} \left( \frac{\Delta K_{th}}{\Delta \sigma_f Y} \right)^2 \quad (11)$$

where  $a_i$  is the EIFS length,  $\Delta \sigma_f$  the fatigue limit,  $\Delta K_{th}$  the intrinsic fatigue threshold stress intensity factor, and  $Y$  is a geometry correction factor.

Eq. (11) is the expression for the proposed EIFS. If the specimen has an initial crack length of EIFS and is under the stress range  $\Delta \sigma_f$ , the fatigue-life prediction using a fracture mechanics-based approach is infinity, which is the experimental fatigue life under fatigue limit.

The material fatigue crack growth curve can be expressed as

$$da/dN = C[\Delta K - \Delta K_{th}]^m \quad (12)$$

where  $C$  and  $m$  are fitting parameters. Eq. (12) can be rewritten as

$$dN = \frac{1}{C[\Delta K - \Delta K_{th}]^m} da \quad (13)$$

Integrating both sides, fatigue life  $N$  can be obtained as

$$N = \int_0^N dN = \int_{a_i}^{a_c} \frac{1}{C[\Delta K - \Delta K_{th}]^m} da \quad (14)$$

where  $a_c$  is the critical length at failure which can be calculated using fracture toughness and applied stress levels.  $a_c$  also depends on the specimen geometry and loading types.  $a_i$  is the EIFS and is determined by Eq. (11).

Plastic deformation of the material is included by considering the crack tip plastic zone as

$$\rho = a \left( \sec \frac{\pi \sigma_{max}(1-R)}{4\sigma_0} - 1 \right) \quad (15)$$

where  $\sigma_0$  is the cyclic ultimate strength, which represents the fatigue strength at one cycle. Considering plastic correction, the stress intensity factor can be expressed as,

$$\Delta K = \sigma_{max} \sqrt{\pi a'} Y' \quad (16)$$

where  $Y'$  is the geometry correction factor using the equivalent crack length  $a'$  considering the plastic correction.  $a'$  can be expressed as

$$a' = a + \rho \quad (17)$$

Detailed derivation and validation for the life prediction methodology can be found in the part I of this paper.

In Section 2.1, the equivalent stress intensity factor under multiaxial loading is developed (Eq. (10)). Eq. (14) is extended

for general multiaxial fatigue-life prediction by replacing the mode I SIF with the equivalent SIF determined by Eq. (12), i.e.

$$N = \int_0^N dN = \int_{a_i}^{a_c} \frac{1}{C[\Delta K_{eq} - \Delta K_{th}]^m} da \quad (18)$$

### 3. Validation of fatigue-life prediction model

#### 3.1. Experimental data

Four sets of experimental fatigue data are employed in this section: Al 7075-T6 [39,40], Ti-6Al-4V [41], 304 stainless steel [42], and SM45C steel [43]. The collected data consists of metallic materials from different industries, such as the automotive and aerospace industry. These experimental also cover different loading conditions, such as proportional and nonproportional loading. A summary of the collected experimental data is listed in Table 2 and different stress paths used in this study are illustrated in Fig. 2.

#### 3.2. Calibration and prediction

In the proposed methodology, crack growth curves under pure mode I and pure mode II load are required (Section 2.1). However, crack growth testing under pure mode II is difficult to perform and the crack growth data under pure mode II loading are rarely found in the literature for many materials. If pure mode II data is not reported, a calibration must be first performed using a mixed-mode crack growth testing or an  $S-N$  curve. In this paper, three types of calibration are used to demonstrate the applicability of the proposed life prediction method.

- (1) No calibration: the crack growth data under both pure mode I and pure mode II are available. For this case, the material parameters  $C$ ,  $m$  required in Eq. (13) can be directly obtained from crack growth curves without calibration. Material Al 7075-T6 collected in this paper belongs to this category.
- (2) Calibration of pure mode II crack growth curve using the mixed-mode crack growth curve data: if pure mode II data is not available but mixed-mode crack growth testing data is available, the pure mode II crack growth data can be calibrated using the method described in Section 2.1. Once the pure mode II crack growth rate is obtained, the fatigue-life prediction can be performed following the same procedure without calibration. SM45C collected in this study belongs to this category.
- (3) Calibration of pure mode II crack growth curve using  $S-N$  curve data: for some materials, only pure mode I crack growth rate curve is available. The crack growth curve under pure mode II load can be calibrated using the experimental  $S-N$  curve under pure torsional loading and the proposed life prediction method. Trial and error method is used for calibration. Materials Ti-6Al-4V and 304 stainless steel collected in this paper belong to this category.

Once the calibration step is finished, all other  $S-N$  data (e.g.  $S-N$  testing data under proportional and nonproportional loading) is used to validate the fatigue-life prediction methodology. To clearly show the prediction capability of the proposed methodology, calibration and prediction data sets are marked in the legend of the validation figures. “Cali” indicates the data is used for calibration and “Pre” indicates the data is only used for prediction.

**Table 2**  
Summary of collected experimental data.

Material	Calibration data	Loading condition	Refs.
AL7075-T6	$da/dN$ for mode I $da/dN$ for mode II	Proportional	[39,40,44,45]
Ti-6Al-4V	$da/dN$ for mode I $S-N$ curve for mode II	Proportional and nonproportional	[41,46]
Type 304 stainless steel	$da/dN$ for mode I $S-N$ curve for mode II	Proportional and nonproportional	[42,47]
SM45C steel	$da/dN$ for mixed-mode	Nonproportional	[43,48]

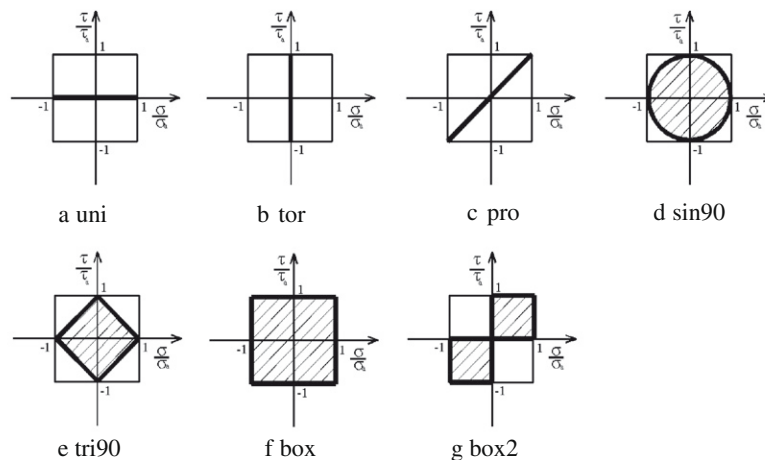


**Fig. 2.** Stress paths used in the current study.

### 3.3. Model validation using experimental data

The predicted fatigue lives and the experimental lives under different loading path, e.g. proportional loading and nonproportional loading, are plotted together in Figs. 3–6. The x-axis is the experimental life and the y-axis is the predicted life, both in log scale.

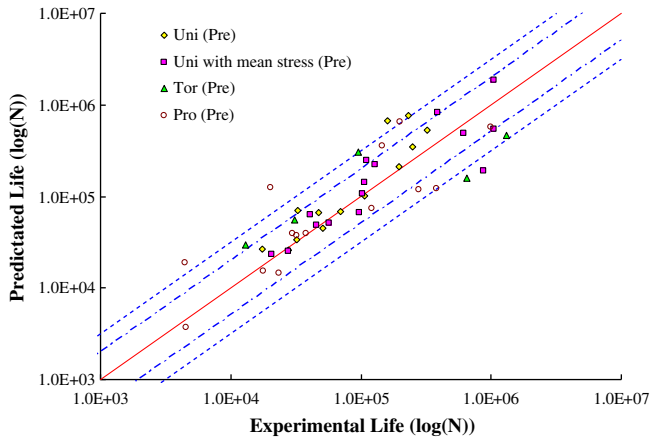


Fig. 3. Comparison of predicted and experimental fatigue lives for Al 7075-T6 [39,40].

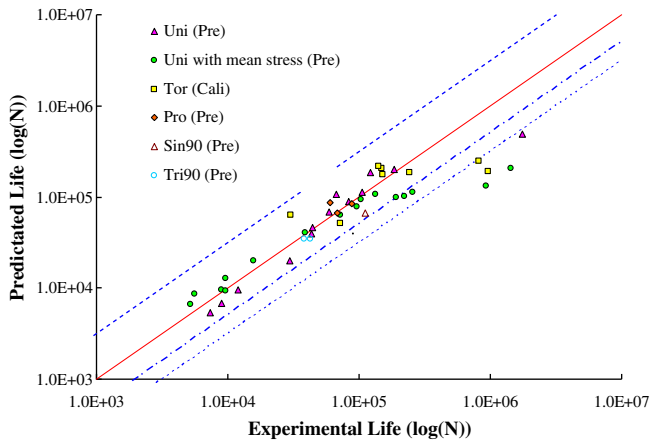


Fig. 4. Comparison of predicted and experimental fatigue lives for Ti-6Al-4V [41].

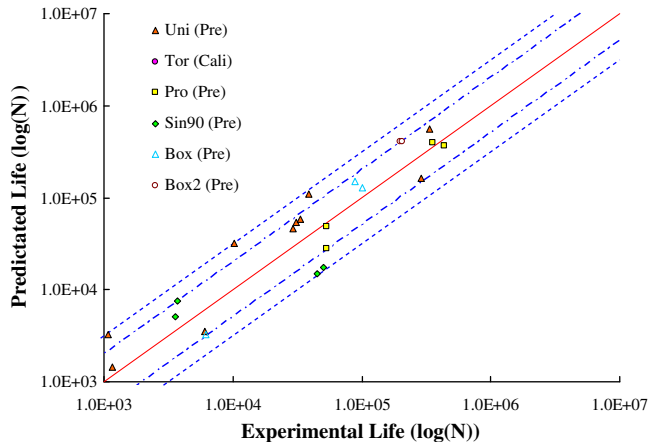


Fig. 5. Comparison of predicted and experimental fatigue lives for type 304 stainless steel [42].

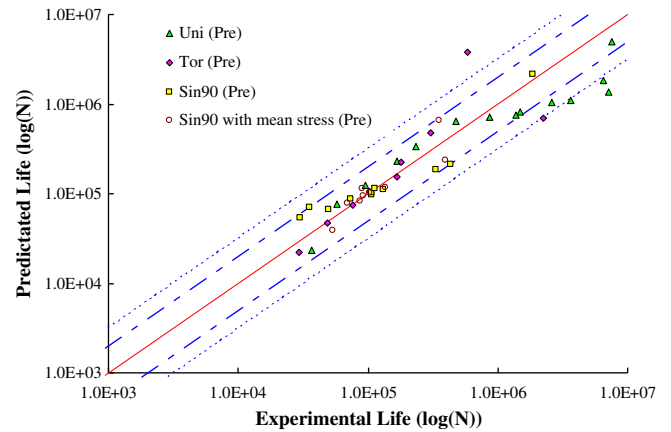


Fig. 6. Comparison of predicted and experimental fatigue lives for SM45C steel [49].

Two bounds are plotted, the inner bound is according to a life factor of two and the outer bound is according to a life factor of three. The different stress paths used in this study and are shown in Fig. 2. In the legend, “Uni” indicates the data is under uniaxial loading and “Tor” indicates the data is under pure torsional loading.

From Figs. 3–6, it is shown that the model prediction results have reasonable agreement with the experimental observations. About 90% of the total points fall into range of life factor three. The validation shows that the proposed model can be used for fatigue-life predictions of smooth specimens under both proportional and nonproportional loading conditions.

As for the initial crack orientation and crack growth orientation from the model prediction have been compared with experimental data in However, for the curvilinear crack growth under general multiaxial variable loading, further theoretical and experimental work are required.

## 4. Conclusions

A new multiaxial fatigue life prediction model, which is based on a critical plane-based model and an EIFS methodology, is developed for multiaxial fatigue-life prediction under constant amplitude fatigue-life prediction under proportional and nonproportional loading conditions. In the proposed model, the critical plane depends on both the stress state and the material properties. The critical plane is theoretically determined by the maximum normal stress plane and the ratio of modes II and I stress intensity factor coefficients  $s$  corresponding to a specific crack growth rate. The critical plane changes corresponding to different material failure modes, thus make the proposed model applicable to a wide range of materials. The used EIFS methodology for fatigue-life prediction unifies the traditionally used fatigue crack initiation and propagation analysis into a single framework and does not require solving the inverse crack growth problems, which makes the computation very efficient and accurate. Comparisons between the predicted fatigue life and the experimental data show strong agreement. Several conclusions can be drawn based on the current study:

- (1) The proposed crack growth-based fatigue-life prediction methodology is applicable for multiaxial loading if the classical Kitagawa diagram is extended to the mode II loading case following the procedures described in this work.
- (2) The proposed methodology requires crack growth rate curves under both modes I and II loading, which can be obtained from direct measurements or from calibrations using other sets of experimental data.

- (3) The current model considers the experimentally observed loading path dependence on the crack growth rate. The experimental data under different paths loadings, e.g. proportional loading and nonproportional loading, are used to validate the proposed model.
- (4) Different uncertainty behavior is observed for the investigated materials and a probabilistic approach may be more suitable to describe the observed uncertainties.

The current investigation only considers smooth specimen life prediction. Further experimental and theoretical work is required for multiaxial fatigue-life prediction of notched specimens. Life prediction under general multiaxial random variable loading needs further investigation as well.

### Acknowledgements

The research reported in this paper was supported by funds from NASA Ames Research Center (Contract No. NNX09AY54A, Project Manager: Dr. Kai Goebel) and by funds from the Federal Aviation Administration William J. Hughes Technical Center (Contract No. DTFAC-06-C-00017, Project Manager: Dr. John Bakuckas). The support is gratefully acknowledged.

### References

- [1] Beranger A-S et al. A fatigue life assessment methodology for automotive components. In: European structural integrity society. Elsevier; 1997. p. 17–25.
- [2] Toor PM. A unified engineering approach to the prediction of multiaxial fatigue fracture of aircraft structures. *Eng Fract Mech* 1975;7(4):731–41.
- [3] Qian J, Fatemi A. Mixed mode fatigue crack growth: a literature survey. *Eng Fract Mech* 1996;55(6):969–90.
- [4] Liu Y, Mahadevan S. A unified multiaxial fatigue damage model for isotropic and anisotropic materials. *Int J Fatigue* 2007;29(2):347–59.
- [5] Liu Y, Mahadevan S. Multiaxial high-cycle fatigue criterion and life prediction for metals. *Int J Fatigue* 2005;27(7):790–800.
- [6] You B-R, Lee S-B. A critical review on multiaxial fatigue assessments of metals. *Int J Fatigue* 1996;18(4):235–44.
- [7] Papadopoulos IV et al. A comparative study of multiaxial high-cycle fatigue criteria for metals. *Int J Fatigue* 1997;19(3):219–35.
- [8] Carpinteri A, Spagnoli A. Multiaxial high-cycle fatigue criterion for hard metals. *Int J Fatigue* 2001;23(2):135–45.
- [9] Wang Y-Y, Yao W-X. Evaluation and comparison of several multiaxial fatigue criteria. *Int J Fatigue* 2004;26(1):17–25.
- [10] Goncalves CA, Araujo JA, Mamiya EN. Multiaxial fatigue: a stress based criterion for hard metals. *Int J Fatigue* 2005;27(2):177–87.
- [11] Gough HJ, Pollard HV. The strength of metals under combined alternating stress. *Proc Inst Mech Eng* 1935;131:3–18.
- [12] Gough HJ, Pollard HV. Properties of some materials for cast crankshafts, with special reference to combined alternating stresses. *Proc Inst Automob Eng* 1937;31:821–93.
- [13] Lee SB. A criterion for fully reversed out-of-phase torsion and bending. In: Miller KJ, Brown MW, editors. *Multiaxial fatigue*, ASTM STP 853. Philadelphia: ASTM; 1985. p. 553–68.
- [14] Sines G. Behaviour of metals under complex stresses. In: Sines G, Waisman JL, editors. *Metal fatigue*. New York: McGraw-Hill; 1959. p. 145–69.
- [15] Sines G. Behaviour of metals under complex stresses. In: Sines J, editor. *Metal fatigue*. New York: McGraw-Hill; 1959. p. 145–69.
- [16] Marin J. Interpretation of fatigue strengths for combined stresses. In: Proceedings of the international conference on fatigue of metals. London: Institution of Mechanical Engineers; 1956.
- [17] Crossland B. Effect of large hydrostatic pressures on the torsional fatigue strength of an alloy steel. In: Proceeding of the international conference on fatigue of metals. London: Institution of Mechanical Engineers; 1956.
- [18] Sines G, Ohgi G. Fatigue criteria under combined stresses or strains. *J Eng Mater Technol* 1981;103:82–90.
- [19] Kakuno H, Kawada K. A new criterion of fatigue strength of a round bar subjected to combined static and repeated bending and torsion. *Fatigue Eng Mater Struct* 1979;2(2):229–36.
- [20] Dietmann H, Bonghibhat T, Schmid A. Multiaxial fatigue behavior of steels under in-phase and out-of-phase loading including different wave forms and frequencies. In: Third international conference on biaxial/multiaxial fatigue. Stuttgart; 1989.
- [21] Sosino CM, Crubisic V. Fatigue behavior of cyclically softening and hardening steels under multiaxial elastic–plastic deformation. In: Miller KJ, Brown MW, editors. *Multiaxial Fatigue*, ASTM STP 853. Philadelphia: American Society for Testing and Materials; 1985. p. 586–605.
- [22] Liu J, Zenner H. Berechnung der Dauerschwingfestigkeit bei mehrachsiger Beanspruchung. *Mater-wiss Werkst* 1993;24(7):240–9.
- [23] Shariyat M. A fatigue model developed by modification of Gough's theory, for random non-proportional loading conditions and three-dimensional stress fields. *Int J Fatigue* 2008;30(7):1248–58.
- [24] Stanfield G. Discussion on the strength of metals under combined alternating stresses. In: Gough H, Pollard H, editors. *Proceedings of the institution of mechanical engineers*; 1935.
- [25] Karolczuk A, Macha E. Selection of the critical plane orientation in two-parameter multiaxial fatigue failure criterion under combined bending and torsion. *Eng Fract Mech* 2008;75(3–4):389–403.
- [26] Findley WN. A theory for the effect of mean stress on fatigue of metals under combined torsion and axial load or bending. *J Eng Ind, Trans ASME* 1959;81:301–6.
- [27] Matak T. An explanation on fatigue limit under combined stress. *Bull JSME* 1977;20:257–63.
- [28] McDiarmid DL. A general criterion for high cycle multiaxial fatigue failure. *Fatigue Fract Eng Mater Struct* 1991;14:429–53.
- [29] Brown MW, Miller KJ. A theory for fatigue failure under multiaxial stress-strain conditions. *Proc Inst Mech Eng* 1973;187:745–55.
- [30] Fatemi A, Socie DF. A critical plane approach to multiaxial fatigue damage including out-of-phase loading. *Fatigue Fract Eng Mater Struct* 1988;11(3):145–65.
- [31] Carpinteri A, Brighenti R, Spagnoli A. A fracture plane approach in multiaxial high-cycle fatigue of metals. *Fatigue Fract Eng Mater Struct* 2000;23(4):355–64.
- [32] Spagnoli A. A new high-cycle fatigue criterion applied to out-of-phase biaxial stress state. *Int J Mech Sci* 2001;43(11):2581–95.
- [33] Liu Y, Mahadevan S. Threshold stress intensity factor and crack growth rate prediction under mixed-mode loading. *Eng Fract Mech* 2007;74(3):332–45.
- [34] Liu Y, Mahadevan S. Probabilistic fatigue life using an Equivalent Initial Flaw Size distribution. *Int J Fatigue* 2009;31(3):476–87.
- [35] Döring R, Hoffmeyer J, Seeger T, Vormwald M. Short fatigue crack growth under nonproportional multiaxial elastic–plastic strains. *Int J Fatigue* 2006;28:972–82.
- [36] Liu Y, Mahadevan S. Stain based multiaxial fatigue damage modeling. *Fatigue Fract Eng Mater Struct* 2005;28:1177–89.
- [37] Kitagawa H, Takahashi S. Applicability of fracture mechanics to very small cracks or cracks in early stage. In: Proceedings of second international conference on mechanical behavior of materials. Metal Park (OH, USA): ASM International; 1976.
- [38] El Haddad MH, Topper T, Smith KN. Prediction of nonpropagating cracks. *Eng Fract Mech* 1979;11:573–84.
- [39] Newman JC, Phillips EP, Swain MH. Fatigue-life prediction methodology using small crack theory. *Int J Fatigue* 1999;21(2):109–19.
- [40] Zhao T, Jiang Y. Fatigue of 7075-T651 aluminum alloy. *Int J Fatigue* 2008;30(5):834–49.
- [41] Kallmeyer Alan R, Krgo Ahmo, Kurath Peter. Evaluation of multiaxial fatigue life prediction methodologies for Ti-6Al-4V. *J Eng Mater Technol* 2002;124(2):229–37.
- [42] Socie D. Multiaxial fatigue damage models. *Eng Mater Technol* 1987;109:293–8.
- [43] Lee SB. Out-of-phase, combined bending and torsion fatigue of steels. In: Miller KJ, Brown MW, editors. *Biaxial and multiaxial fatigue*. London: Mechanical Engineering Publications; 1989. p. 621–41.
- [44] Tanaka K, Matsuoka S, Kimura M. Fatigue strength of 7075-T6 aluminium alloy under combined axial loading and torsion. *Fatigue Eng Mater Struct* 1984;7(3):195–211.
- [45] Zhao T, Zhang J, Jiang Y. A study of fatigue crack growth of 7075-T651 aluminum alloy. *Int J Fatigue* 2008;30(7):1169–80.
- [46] Ritchie RO et al. Thresholds for high-cycle fatigue in a turbine engine Ti-6Al-4V alloy. *Int J Fatigue* 1999;21(7):653–62.
- [47] Tsay LW et al. The effect of sensitization on the hydrogen-enhanced fatigue crack growth of two austenitic stainless steels. *Corros Sci* 2008;50(5):1360–7.
- [48] You BR, Lee SB. Fatigue crack growth behaviour of SM45C Steel under mixed-mode I and II loading. *Fatigue Fract Eng Mater Struct* 1998;21:1037–48.
- [49] Kurath P, Downing SD, Galliar DR. Summary on non-hardened notched shaft round robin program. In: Lees GE, Socie DF, editors. *Multiaxial fatigue: analysis and experiments*. SAE; 1989. p.13–31.